

Tunneling in proton glasses: Stochastic theory of NMR line shape

S. Dattagupta

School of Physical Sciences, Jawaharlal Nehru University, New Delhi 110067, India

B. Tadić, R. Pirc, and R. Blinc

Jožef Stefan Institute, 61111 Ljubljana, Yugoslavia

(Received 21 March 1991)

The effects of the tunneling motion of hydrogen on the NMR line shape in randomly mixed ferroelectric crystals of the type $\text{Rb}_{1-x}(\text{NH}_4)_x\text{H}_2\text{PO}_4$, known as proton glasses, is studied. The line shapes are calculated for the Clausen-Blume model with use of mean-field theory applied to the infinite-range model of an Ising spin glass in a transverse field, which describes the tunneling frequency of a proton in the $\text{O}-\text{H}\cdots\text{O}$ bond. The interplay of tunneling and spin-glass-like ordering phenomena leads to characteristic features in the NMR, NQR, and EPR spectral line shapes. Magnetic-resonance line-shape measurements thus permit discrimination between coherent tunneling processes and classical thermally activated intrabond hopping across the potential barrier in proton glasses.

I. INTRODUCTION

Randomly mixed hydrogen bonded ferroelectric and antiferroelectric crystals such as $\text{Rb}_{1-x}(\text{NH}_4)_x\text{H}_2\text{PO}_4$, known as RADP, and its deuterated counterpart D-RADP have attracted a great deal of both experimental¹⁻⁴ and theoretical⁵⁻¹³ attention in recent years. These proton and deuteron glasses are different from ordinary glasses as they are characterized by solid-solid phase transitions. On the other hand, they may be viewed as akin to magnetic spin glasses.¹⁴ This is so because the underlying lattice structure of proton glasses remains crystalline, whereas randomness is caused by an admixture of ferroelectric and antiferroelectric bonds, leading to both quenched disorder and frustration. A systematic study of RADP and D-RADP crystals is thus expected to throw some light not only on the rich and intricate physics of the glass transition but also on the fascinating new kind of statistical mechanics that is involved in disordered systems.¹⁵

In one respect, however, the above mixed crystals are different from the usual spin glasses. They are governed not just by the presence of bond disorder but also by random local fields caused by substitutional disorder. The latter feature makes these systems quite distinct from other dilute magnetic systems where the random fields are generated by the application of external magnetic fields. The interplay of both bond disorder and random fields has already been the subject of extensive investigation in D-RADP crystals.^{1,2}

Our main interest in the present paper is in undeuterated RADP-like systems where the quantum dynamics of the proton lends additional features to the systems. The “left” and “right” positions of the proton in an $\text{O}-\text{H}\cdots\text{O}$ bond are mapped onto an Ising pseudospin variable S^z which may take on values $+1/2$ and $-1/2$. The Hamil-

tonian of interaction between two protons separated by distances much larger than the bond length is governed by the usual exchange couplings and local fields. Thus the above model is equivalent to an Ising spin glass in a random field and is appropriately referred to as a proton glass. However, unlike the deuteron (in D-RADP), the proton can tunnel between its left and right positions. As this motion is governed by quantum laws and not thermal activation, it persists down to zero temperature, and requires a modification of the Ising Hamiltonian.¹⁶

Although at first sight the proton glass may appear to be a hopelessly complicated system in which one has to deal with not only random exchange and random fields but quantum effects as well, there is one simplified aspect that makes it amenable to theoretical studies. This is the fact that, in spin glasses and related systems, mean-field theory (MFT) based on the infinite-range random-bond model provides a good description of the relevant physics.^{17,18} In what follows, therefore, we shall assume the validity of MFT at the outset, in determining both static and dynamic properties of proton glasses.

One of the most accurate tools for the study of proton and deuteron dynamics in hydrogen bonded glasses is provided by the techniques of nuclear magnetic resonance (NMR) and nuclear quadrupole resonance (NQR).¹⁹ In this, one derives the advantage of a “local” probe which is also extremely sensitive. Our principal aim in this paper is to present a theory of the magnetic resonance line shapes so as to bring out the salient features of disorder and tunneling. The hope is to construct a theory that is intuitive and mathematically simple, in order to facilitate a systematic comparison with experimentally observed line shapes in proton glasses. One such theory based on stochastic considerations and developed by Kubo,²⁰ Anderson²¹ and others,¹⁹ has been popular for more than three decades. The Kubo-Anderson model as-

sumes a discrete jump process by which the resonant frequency jumps at random from one value to another with a probability determined by detailed balance of transitions at finite temperatures.²² When it comes to proton glasses, however, the Kubo-Anderson model has to be generalized in order to incorporate the quantum effects of tunneling. Such a generalization, in which a part of the system, called a subsystem, is treated quantum mechanically, while the surrounding heat bath is handled as a classical stochastic reservoir, was carried out by Blume²³ and co-workers.^{24,25} We adopt here the Clauser-Blume model for making an explicit line-shape calculation applicable to proton glasses. In this, the subsystem is governed by a quantum Hamiltonian for the pseudospins, embedded in an effective medium characterized by “mean” fields, and subject to fluctuations driven by a classical heat bath.

With the preceding remarks about the purpose and the scope of the present investigation, the outline of the paper is as follows. In Sec. II, we present the line-shape expression and also the basic Hamiltonian. We then cast the line shape within the context of the Clauser-Blume model. In Sec. III, we put forward the physical basis of our proposed model for the relaxational dynamics induced by the heat bath. Based on this model, the underlying correlation function is calculated in Sec. IV, and the limit of zero tunneling is recovered. Our main results for the magnetic resonance line shape are then presented in Sec. V. Finally, in Sec. VI we indicate the possibility of comparing the derived expressions with experiments, and also present our principal conclusions.

II. THE LINE SHAPE AND DISORDER-AVERAGED CORRELATION FUNCTION

In Fig. 1 we show schematically an O—H···O-type double-well potential, in which the proton moves. The parameters of the potential and the temperature are such that the proton spends most of its time at the bottom of either the left or the right well and very little time in between. One then essentially has a two-level

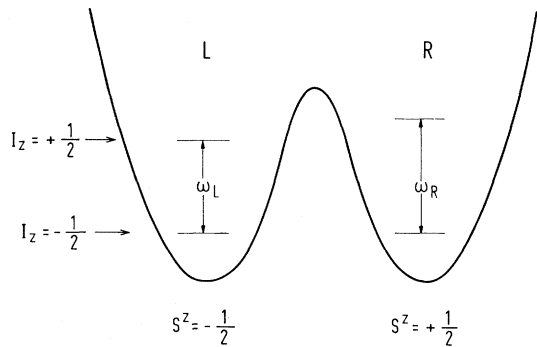


FIG. 1. Double-well potential of a proton in the O—H···O bond.

system²⁶ (TLS) defined in terms of the pseudospin variables $S^z = \pm 1/2$, which designate the left or right positions of the proton in the double well. As the proton moves from the left to the right well, the NMR, NQR, or EPR resonant frequency is assumed to jump from ω_L to ω_R , and vice versa. While ω_L and ω_R can be multivalued, we assume without loss of generality that there is just one value of the NMR, NQR, or EPR frequency in either well. Thus the frequencies ω_L and ω_R can be seen to occur as a result of transitions between the eigenstates of a spin-half operator,²⁷ denoted here by $I^z = \pm 1/2$, and the spin Hamiltonian can be constructed as

$$H = \bar{\omega} I^z + \Delta\omega I^z S^z, \quad (2.1)$$

where

$$\bar{\omega} = \frac{1}{2}(\omega_L + \omega_R), \quad \Delta\omega = \omega_R - \omega_L. \quad (2.2)$$

The resonance transitions in the Hilbert space of the I spin are caused by the raising and the lowering operators I^+ and I^- . The line shape is then given by²²

$$J(\omega) = \frac{1}{\pi} \text{Re} \int_0^\infty dt \exp(-i\omega t) C(t), \quad (2.3)$$

where the correlation function $C(t)$ is defined as

$$C(t) = \langle I^-(0) I^+(t) \rangle. \quad (2.4)$$

Here the angular brackets denote the appropriate quantum and statistical average, and $I^\pm(t)$ are the operators I^\pm in the Heisenberg picture:

$$I^\pm(t) = \exp(iHt) I^\pm(0) \exp(-iHt). \quad (2.5)$$

It is easy to see that in the case of Eq. (2.1), the correlation function is given by

$$C(t) = \langle \exp[it(\bar{\omega} + \Delta\omega S^z)] \rangle, \quad (2.6)$$

after having carried out the trace over the quantum states of I^z . The angular brackets in Eq. (2.6) then denote the remaining average to be done over the states of S^z . If $S^z(t)$ is assumed to be governed by a classical stochastic process due to the dynamics induced by heat bath, Eq. (2.6) may be written as

$$C(t) = \left[\exp i \left(\bar{\omega} t + \Delta\omega \int_0^t S^z(t') dt' \right) \right]_{\text{av}}, \quad (2.7)$$

where $[\dots]_{\text{av}}$ denotes a stochastic average. Equation (2.7) forms the starting point of the analysis by Pirc *et al.*¹²

Having formulated the line shape for an isolated doublewell in the absence of tunneling, we now include the interwell interaction and the possibility of tunneling between two proton sites in the O—H···O bond. The Hamiltonian in Eq. (2.1) is then to be generalized to the form

$$H = \bar{\omega} \sum_i I_i^z + \Delta\omega \sum_i I_i^z S_i^z - \frac{1}{2} \sum_{i,j} J_{ij} S_i^z S_j^z - \Omega \sum_i S_i^x - \sum_i f_i S_i^z, \quad (2.8)$$

where the last three terms describe the interacting pseudospin system.⁵

Furthermore, J_{ij} is the infinite-ranged quenched random interaction between the pseudospins S_i^z , Ω/\hbar is the tunneling frequency, and f_i represents the random longitudinal field at site i . The random interactions J_{ij} and the fields f_i are assumed to be independently distributed according to their respective Gaussian probability distributions:

$$P(J_{ij}) = \frac{1}{\sqrt{2\pi J^2}} \exp\left(-\frac{J_{ij}^2}{2J^2}\right), \quad (2.9)$$

$$P(f_i) = \frac{1}{\sqrt{2\pi\Delta}} \exp\left(-\frac{f_i^2}{2\Delta}\right). \quad (2.10)$$

In what follows, we shall denote by $[\dots]_d$ an average with respect to combined distributions (2.9) and (2.10). Both J^2 and Δ depend on the concentration x characterizing the composition of the proton glass as in the case $\text{Rb}_{1-x}(\text{NH}_4)_x\text{H}_2\text{PO}_4$. The simplest concentration dependence has the form

$$\Delta = 4x(1-x)\Delta_{\max}, \quad (2.11)$$

and a similar relation can be assumed for the variance J^2 .

Note that in spin-glass theories one usually employs an Ising variable $S^z = \pm 1$ rather than the pseudospin $S^z = \pm 1/2$. Therefore, the parameters Ω , J , and Δ of Ref. 11 are replaced by $\Omega/2$, $J/4$, and $\Delta/4$, respectively, in the present case. As mentioned earlier, we shall treat the pseudospin system within the framework of a MFT of quantum spin glasses. As a first step we shall replace the Hamiltonian (2.8) by an effective Hamiltonian

$$H_{\text{MFT}} = \bar{\omega} \sum_i I_i^z + \Delta\omega \sum_i I_i^z S_i^z - \sum_i h_i S_i^z - \Omega \sum_i S_i^x, \quad (2.12)$$

where h_i represents an effective field at site i to be specified below. Equation (2.12) can be further simplified by noting that $\bar{\omega}$ can be absorbed in the frequency factor ω in Eq. (2.3).

A systematic MFT for the model of a quantum glass defined by Eqs. (2.12), (2.9), and (2.10) has been carried out in Ref. 11 using the thermofield-dynamic approach³¹ and the instantaneous approximation for the dynamic self-interaction. The effective single-spin Hamiltonian has been derived, which, together with the term representing interaction with the surrounding medium, can be written as

$$H_0 = \Delta\omega I^z S^z - hS^z - \Omega S^x. \quad (2.13)$$

Here $h = h(z)$ is an effective field acting on the pseudospin along the z axis due to a nonzero spin-glass order parameter ($q \neq 0$),

$$h(z) = \frac{1}{2}J\sqrt{q + \tilde{\Delta}z}, \quad (2.14)$$

where z is a Gaussian noise field and $\tilde{\Delta} \equiv 4\Delta/J^2$. Thus the total field has a strength

$$h_0(z) = \sqrt{\Omega^2 + h(z)^2}. \quad (2.15)$$

In the static limit the mean-field equations for the local polarization $p(z)$ and the spin-glass order parameter q are obtained as¹¹

$$p(z) = r(z) \tanh\left(\frac{1}{2}\beta h_0(z)\right) \quad (2.16)$$

and

$$q = \int_{-\infty}^{+\infty} \frac{dz}{\sqrt{2\pi}} e^{-\frac{1}{2}z^2} p(z)^2, \quad (2.17)$$

where

$$r(z) = \frac{h(z)}{h_0(z)}. \quad (2.18)$$

The Hamiltonian in Eq. (2.13) still describes the static properties of the system only. In accordance with our stated objective we now assume that the system described by H_0 is placed in a contact with a heat bath.²⁴ The latter is characterized by "stochastic forces," which cause transitions between quantum states of H_0 . In order to incorporate this physics into our formalism, we first note that the line shape can be written as [cf. Eq. (2.3)]

$$J(\omega) = \frac{1}{\pi} \text{Re}[\hat{C}(s)]_d, \quad s = i\omega, \quad (2.19)$$

where $\hat{C}(s)$ is the Laplace transform of $C(t)$ and $[\dots]_d$ is the disorder average. From Eqs. (2.4) and (2.5), $\hat{C}(s)$ can be expressed as

$$\hat{C}(s) = \langle I^-(0) \{ [\hat{U}(s)]_{\text{av}} I^+(0) \} \rangle, \quad (2.20)$$

where $[\hat{U}(s)]_{\text{av}}$ denotes the Laplace transform of the averaged time development operator of the system.²²⁻²⁵ The angular brackets in Eq. (2.20) indicate the average over the quantum states of H_0 . In the Clauser-Blume model²⁴

$$[\hat{U}(s)]_{\text{av}} = [s - iH_0^X - \lambda(J_{\text{av}} - 1)]^{-1}, \quad (2.21)$$

where H_0^X is the Liouville operator associated with H_0 , λ is a phenomenological parameter called the relaxation rate, and J_{av} is an average transition operator. The idea behind Eq. (2.21) is clear: if there is no coupling to the heat bath, J_{av} is unity and the time evolution is totally dictated by H_0^X alone. It is now left to model J_{av} in such a way that the heat-bath-driven transitions in the S system do not disturb the net thermal equilibrium, i.e., detailed balance is preserved. We shall follow in the sequel the notations used in Ref. 22, wherein Eq. (2.21) has been derived under the assumption of what is called an impulse process.

III. MODEL FOR THE TRANSITION OPERATOR

As noted earlier, the operator J_{av} contains all the information concerning the dynamic effects of the heat bath. In the usual treatments of mixed crystals, in the absence of the tunneling term, i.e., $\Omega = 0$, it is customary to

imagine that the dynamics arise from additional coupling terms to the heat bath, added onto Eq. (2.8), which are off diagonal in the representation in which S^z is diagonal. This is then in the spirit of the kinetic Ising model of the Glauber type.²⁸ Within this model an expression for the line shape has been recently derived by Pirc *et al.*,¹² using a path-integral formulation of the spin-glass problem.²⁹ The physical meaning of the Glauber terms is evident: they cause spontaneous spin-flips, which, in the context of causal systems, mimick thermally activated jumps of the proton or deuteron between the two sites in the O—H···O or O—D···O bonds, respectively.

In the case in which $\Omega \neq 0$, we could still imagine the heat bath interactions to be of the Glauber type. But that would be tantamount to taking into account only the classically activated jump processes. In reality we expect the heat bath to induce not only thermal fluctuations of the above kind, but quantum fluctuations as well, leading to “incoherence” in tunneling, which is otherwise a coherent phenomenon. An extensive study of such dissipative effects in a quantum TLS has recently been made and comprehensively reviewed in Ref. 26. In the latter the coupling to the heat bath is taken to be proportional to S^z . This is, again, not adequate for our purpose as we would like to recover the Glauber mechanism in the limit $\Omega = 0$. The point is, when $\Omega \neq 0$, the appropriate quantization axis is neither z nor x , but it is somewhere inbetween. The simplest coupling to the heat bath would then be proportional to an operator that is strictly off-diagonal in the new representation of the quantization axis, and would lead to correct limits when either (i) $\Omega = 0$ or (ii) $h = 0$. The required diagonalization of H_0 (actually a partial one) can be simply carried out by performing a rotation in the “spin space” of the S system by an angle $\theta = \text{arctanh}(\Omega/h)$ from the x to the x' frame around the y axis. In the rotated frame the Hamiltonian H_0 reads

$$\tilde{H}_0 = I^z(a_1 S^{z'} + a_2 S^{x'}) - h_0 S^{z'}, \quad (3.1)$$

where

$$a_1 = \Delta\omega \frac{h}{h_0}; \quad a_2 = \Delta\omega \frac{\Omega}{h_0}; \quad h_0 = \sqrt{h^2 + \Omega^2}. \quad (3.2)$$

As the correlation function is invariant under such a rotation, the expressions in Eqs. (2.20) and (2.21) would continue to be valid with H_0 replaced by \tilde{H}_0 .

We are now ready to write down the matrix elements of the transition operator J_{av} . Introducing the eigenstates of $S^{z'}$ as $|\mu\rangle, |\nu\rangle$, etc., i.e.,

$$S^{z'}|\mu\rangle = \mu|\mu\rangle, \quad (3.3)$$

and recalling that J_{av} is a superoperator,²² the required elements are

$$(\mu\nu|J_{\text{av}}|\mu'\nu') = p_{\mu'}\delta_{\mu\nu}\delta_{\mu'\nu'}, \quad (3.4)$$

where p_{μ} is the Boltzmann factor in equilibrium, appro-

priate to \tilde{H}_0 . That is,

$$p_{\mu} = \frac{1}{Z_0} \langle \mu | \exp(-\beta \tilde{H}_0) | \mu \rangle, \quad (3.5)$$

Z_0 being the relevant partition function and β the inverse temperature. Since, usually, $1 \gg |\beta \Delta\omega|$, we have from Eq. (3.1),

$$p_{\mu} \approx \exp(\beta h_0 \mu) [2 \cosh(\frac{1}{2} \beta h_0)]^{-1}. \quad (3.6)$$

The form given in Eq. (3.4) is quite general for the spin-half operator, and it is also consistent with detailed balance of transitions at finite temperatures.^{22–25}

IV. CORRELATION FUNCTION

The first step in evaluating the right hand side of Eq. (2.20) is to formally carry out the trace over the eigenstates of I^z and $S^{z'}$. Using the fact that \tilde{H}_0 is diagonal in the representation of I^z and the raising and lowering operators I^{\pm} do not act on the eigenstates of $S^{z'}$, we can show²² that

$$\hat{C}(s) = (+ - | \tilde{U}(s) | + -), \quad (4.1)$$

where

$$\tilde{U}(s) = \sum_{\mu, \nu} p_{\nu} (\nu\nu | \hat{U}(s) | \mu\mu), \quad (4.2)$$

and $|+ -\rangle$ denotes an “eigenvector” of $(I^z)^{\times}$.

The task of computing $\tilde{U}(s)$ is facilitated by the special structure of J_{av} given in Eq. (3.4). Employing a slight generalization of the derivation given in Sec. X.3.2. of Ref. 22, we can show that

$$\tilde{U}(s) = \frac{\tilde{U}_0(s + \lambda)}{1 - \lambda \tilde{U}_0(s + \lambda)}, \quad (4.3)$$

where

$$\tilde{U}_0(s + \lambda) = \sum_{\mu, \nu} p_{\nu} (\nu\nu | [s + \lambda - i\tilde{H}_0^{\times}]^{-1} | \mu\mu). \quad (4.4)$$

Because \tilde{H}_0 involves only I^z , a diagonal operator in I space, we have, from Eqs. (4.1) – (4.4),

$$\hat{C}(s) = \frac{\hat{G}_0(s + \lambda)}{1 - \lambda \hat{G}_0(s + \lambda)}, \quad (4.5)$$

where

$$\hat{G}_0(s + \lambda) = (+ - | \tilde{U}_0(s + \lambda) | + -). \quad (4.6)$$

In order to determine $\hat{G}_0(s + \lambda)$ we need to compute the inverse of the Liouville operator given inside the square brackets in Eq. (4.4). This can be achieved by formally inverting the Laplace transform and writing $\hat{G}_0(s + \lambda)$ as

$$\begin{aligned}\hat{G}_0(s + \lambda) &= \sum_{\mu, \nu} p_\nu \int_0^\infty dt \exp[-(s + \lambda)t] \langle +\nu, -\nu | \exp(i\tilde{H}_0^\times t) | +\mu, -\mu \rangle \\ &= \sum_{\mu, \nu} p_\nu \int_0^\infty dt \exp[-(s + \lambda)t] \langle +\nu | \exp(i\tilde{H}_0 t) | +\mu \rangle \langle -\mu | \exp(-i\tilde{H}_0 t) | -\nu \rangle,\end{aligned}\quad (4.7)$$

where the labels \pm in $|+\mu, -\mu\rangle$, etc., refer to the eigenstates of I^z , and in the last step we have employed the properties of Liouville operators.²² Note that

$$\langle +\nu | \exp(i\tilde{H}_0 t) | +\mu \rangle = \langle \nu | \exp[it(\frac{1}{2}a_1 S^{z'} + \frac{1}{2}a_2 S^{x'} - h_0 S^{z'})] | \mu \rangle. \quad (4.8)$$

The exponential operators on the right-hand side of Eq. (4.8) can be further decomposed by using the properties of spin- $\frac{1}{2}$ matrices.³⁰ Collecting all the matrix elements, doing the integral over t and summations over ν and μ , and after some algebra, we finally obtain

$$\hat{G}_0(s + \lambda) = \frac{s + \lambda + \frac{1}{2}i\tilde{p}a_1}{D_+ D_-} [(s + \lambda)^2 + h_0^2], \quad (4.9)$$

where

$$A_\pm = \sqrt{\left(\frac{1}{2}a_1 \pm h_0\right)^2 + \frac{1}{4}a_2^2}, \quad (4.10)$$

$$D_\pm = (s + \lambda)^2 + \frac{1}{4}(A_+ \pm A_-)^2.$$

The parameter \tilde{p} is the net polarization in the rotated frame. We find

$$\tilde{p} = p_+ - p_- = \tanh(\frac{1}{2}\beta h_0). \quad (4.11)$$

Using the expressions (4.10) and the fact that the polarization p in the laboratory frame is given by $p = (h/h_0)\tilde{p}$, we find that the expression (4.9) can be written as

$$\hat{G}_0(s + \lambda) = \frac{s + \lambda + \frac{1}{2}ip\Delta\omega}{(s + \lambda)^2 + \frac{1}{4}(\Delta\omega)^2 M(s + \lambda)}. \quad (4.12)$$

Here $h_0^2 = h^2 + \Omega^2$ and

$$M(s + \lambda) = \frac{(s + \lambda)^2 + h^2}{(s + \lambda)^2 + h_0^2}. \quad (4.13)$$

Now, from Eq. (4.5) together with Eq. (4.12) we have the following expression for the correlation function:

$$\hat{C}(s) = \frac{s + \lambda + \frac{1}{2}ip\Delta\omega}{s(s + \lambda) - \frac{1}{2}i\lambda p\Delta\omega + \frac{1}{4}(\Delta\omega)^2 M(s + \lambda)}. \quad (4.14)$$

As noted earlier, in the case of deuterated samples such as D-RADP, the quantum tunneling is suppressed and one essentially has a classical problem. When $\Omega = 0$ we have $h_0 = h$, and the Hamiltonian (2.13) reduces to

$$\tilde{H}_0 = H_0 = \Delta\omega I^z S^z - hS^z, \quad (4.15)$$

and

$$\tilde{p} = p = \tanh(\frac{1}{2}\beta h). \quad (4.16)$$

Equation (4.14) then yields

$$\hat{C}(s) = \frac{s + \lambda + \frac{1}{2}ip\Delta\omega}{s(s + \lambda) + \frac{1}{4}(\Delta\omega)^2 - \frac{1}{2}i\lambda p\Delta\omega}. \quad (4.17)$$

Recalling that the Laplace transform variable is $s = i\omega$, we have from Eq. (2.19) the following expression for the line shape:

$$J(\omega) = \frac{1}{4\pi} \int_{-1}^{+1} dp W(p) \frac{\lambda(\Delta\omega)^2(1 - p^2)}{[\omega^2 - \frac{1}{4}(\Delta\omega)^2]^2 + \lambda^2(\omega - \frac{1}{2}p\Delta\omega)^2}. \quad (4.18)$$

The integral over p along with the weight factor $W(p)$, which is defined as

$$W(p) = [\delta(p - 2\langle S^z \rangle)]_d, \quad (4.19)$$

in Eq. (4.18) accounts for the average over quenched disorder.⁶ It should be noted that due to the substitutional disorder and the resulting presence of random local fields, the spin-glass-like order ($q \neq 0$) is present at all temperatures and the local polarization distribution $W(p)$ is nontrivial.³² The formula (4.18) is identical to the one recently derived in a path-integral formulation of the Glauber kinetics²⁹ by Pirc *et al.*,¹² who also provide an expression for $W(p)$ within the same formalism. In the present quantum model we have separated the problems of evaluating the local polarization distribution $W(p)$ and

the correlation function $\hat{C}(s)$. We have calculated $\hat{C}(s)$ within the stochastic model of Clausen and Blume, in which the MFT is built in at the outset, as mentioned before. This strategy is more convenient for attacking the $\Omega \neq 0$ case, as we shall see in the next section. It should be mentioned that for $\Omega = 0$ the Clausen-Blume model reduces to the so-called secular case and becomes equivalent to the classical Kubo-Anderson model. Thus, the result (4.17) could have also been derived independently from the classical model,¹⁹ as can be verified by a direct comparison with Eq. (VIII.49) of Ref. 22. Note, however, that a systematic derivation of $J(\omega)$ in Ref. 12 allows for higher-order corrections which arise due to nonlinearity of the spin-glass dynamics. An equivalent approach in the quantum case is not known so far.

V. LINE SHAPE IN PROTON GLASSES

In the general case when the tunneling term is nonzero, the correlation function $\hat{C}(s)$ is given by the expression (4.14). Let us consider first a somewhat simplified case. Observe that for $\Omega \ll h$, we have $a_1 \approx \Delta\omega$ and $a_2 \approx 0$, whereas for $\Omega \gg h$ one finds $a_1 \approx 0$ and $a_2 \approx \Delta\omega$. Thus, in either case both a_1 and a_2 are at most of order $\Delta\omega$, and hence are much smaller than h_0 itself. To lowest order a_2 may be dropped out, since it appears in Eq. (4.9) only quadratically. This is equivalent to approximating \tilde{H}_0 in Eq. (3.1) by

$$\tilde{H}_0 \approx \frac{h}{h_0} \Delta\omega I^z S^z - h_0 S^z. \quad (5.1)$$

Here h is the effective field along the z axis, which can be determined by using the MFT appropriate for proton glasses, and $h_0 = \sqrt{h^2 + \Omega^2}$, as discussed above.

Comparing Eq. (5.1) with (4.15), it is obvious that we may directly transcribe the expression for the correlation function from Eq. (4.17), provided that we replace the polarization in the laboratory frame p by the polarization in rotated frame \tilde{p} , and $\Delta\omega$ by $(h/h_0)\Delta\omega$. On the other

hand, the polarization in the laboratory frame is given by

$$p = \frac{h}{h_0} \tilde{p} = r \tanh\left(\frac{1}{2}\beta h_0\right), \quad (5.2)$$

where we used Eq. (4.11) and $r = h/h_0$ as in Eq. (2.18). Thus, with the help of these remarks and using Eqs. (2.19) and (4.17) we find the compact expression for the line shape

$$J(\omega) = \frac{1}{4\pi} \left[\frac{\lambda(\Delta\omega)^2 (r^2 - p^2)}{\left[\omega^2 - \frac{1}{4}(r\Delta\omega)^2\right]^2 + \lambda^2(\omega - \frac{1}{2}p\Delta\omega)^2} \right]_d. \quad (5.3)$$

Again, $[\dots]_d$ represents the disorder average.

Using the expressions (2.14) – (2.16), we see that the remaining average over z in (5.3) has to be performed. This is formally equivalent to averaging over the local-polarization distribution $W(p)$, defined in (4.19), since the local polarization p is z dependent in view of Eq. (2.16). Thus we have

$$J(\omega) = \frac{1}{4\pi} \int_{-1}^{+1} dp W(p) \frac{\lambda(\Delta\omega)^2 [r^2(z_0) - p^2]}{\{\omega^2 - [\frac{1}{2}r(z_0)\Delta\omega]^2\}^2 + \lambda^2(\omega - \frac{1}{2}p\Delta\omega)^2}. \quad (5.4)$$

The local-polarization distribution $W(p)$ has been recently calculated within the thermofield-dynamic approach in Ref. 13. The result for the case $S^z = \pm 1/2$ is

$$W(p) = \frac{4e^{-\frac{1}{2}z_0^2}}{\beta J \sqrt{q + \tilde{\Delta}}} \left(r(z_0)^2 + \frac{2\Omega^2}{\beta h(z_0)[h_0(z_0)]^2} p - p^2 \right)^{-1}, \quad (5.5)$$

where $z_0 = z_0(p)$ is the solution of Eq. (2.16).

Considering next the complete expression for $\hat{C}(s)$ given by Eq. (4.14), we find the line shape $J(\omega)$ in units of $\Delta\omega/2$ as follows:

$$J(\omega) = \frac{1}{\omega_1 \pi} \int_{-1}^{+1} dp W(p) \frac{R - p^2 + \gamma^{-1} I(\omega + p)}{(\omega^2 - R)^2 + \gamma^2 (\omega - p + \gamma^{-1} I)^2}, \quad (5.6)$$

where $\omega_1 \equiv \Delta\omega/2$ and we have introduced a dimensionless frequency $\omega \rightarrow \omega/\omega_1$ and relaxation rate $\gamma = \lambda/\omega_1$, while R and I are given by the following expressions:

$$R = 1 - X^2 \tilde{\Omega}^2 \frac{\gamma^2 - \omega^2 + X^2 \left((q + \tilde{\Delta})z^2 + \tilde{\Omega}^2 \right)}{\{\gamma^2 - \omega^2 + X^2 [(q + \tilde{\Delta})z^2 + \tilde{\Omega}^2]\}^2 + 4\gamma^2 \omega^2}, \quad (5.7)$$

and

$$I = 2\tilde{\Omega}^2 X^2 \frac{\gamma\omega}{\{\gamma^2 - \omega^2 + X^2 [(q + \tilde{\Delta})z^2 + \tilde{\Omega}^2]\}^2 + 4\gamma^2 \omega^2}. \quad (5.8)$$

Here we have introduced the dimensionless tunneling frequency $\tilde{\Omega} = 2\Omega/J$ and a parameter X , which represents the ratio of the width of random interaction distribution J and the dynamic parameter $\Delta\omega$, i.e., $X = J/\Delta\omega$.

It should be noted that the Eq. (5.3) can be obtained

as the large- X limit of the Eq. (5.6). In the limit $\Omega \rightarrow 0$, Eq. (5.6) reduces to the well-known expression for the line shape in deuteron glasses obtained earlier.¹² Another interesting feature is obtained for large values of γ . In the limit $\gamma \rightarrow \infty$, referred to as the fast motion limit, where the measuring frequency is much lower than the characteristic frequency for pseudospin flips, Eq. (5.6) reduces to $(1/\omega_1)W(\omega/\omega_1)$, with $W(p)$ given in Eq. (5.5). The results of a numerical evaluation of the line shape given by Eq. (5.6), and using Eqs. (5.5), (5.7), and (5.8) are presented in Figs. 2, 3, and 4 for a fixed value of $X = 10^2$ and for various values of the parameters $\tilde{\Omega}$, $\tilde{\Delta}$, γ ,

and the reduced temperature T/T_0 , where $T_0 \equiv J/4$. In Fig. 5 the line shape is presented for various values of the parameter X with the other parameters being kept fixed at their representative values.

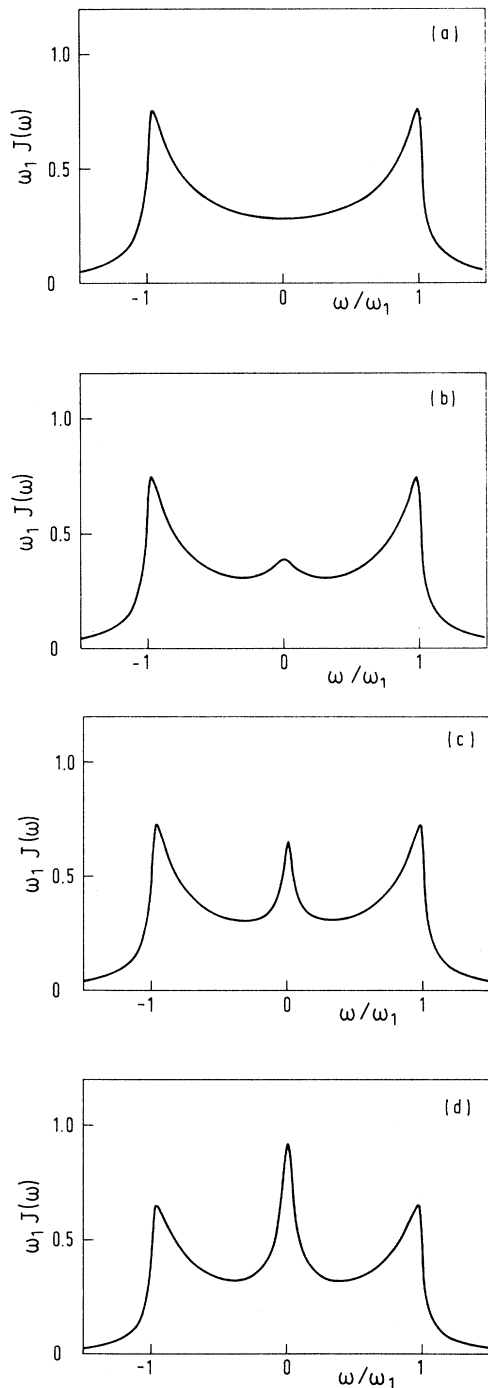


FIG. 2. Line shape $J(\omega)$ plotted vs reduced frequency ω/ω_1 for fixed temperature $T/T_0 = 1.0$, random-field distribution $\tilde{\Delta} \equiv 4\Delta/J^2 = 0.35$, relaxation rate $\gamma \equiv \lambda/\omega_1 = 2.0$, and $X \equiv J/2\omega_1 = 10^2$, and different values of the tunneling frequency $\tilde{\Omega} \equiv 2\Omega/J$: 0.0 (a), 0.05 (b), 0.1 (c), and 0.25 (d).

VI. DISCUSSION AND CONCLUSIONS

The above treatment represents an extension of the stochastic Kubo-Anderson approach for the calculation

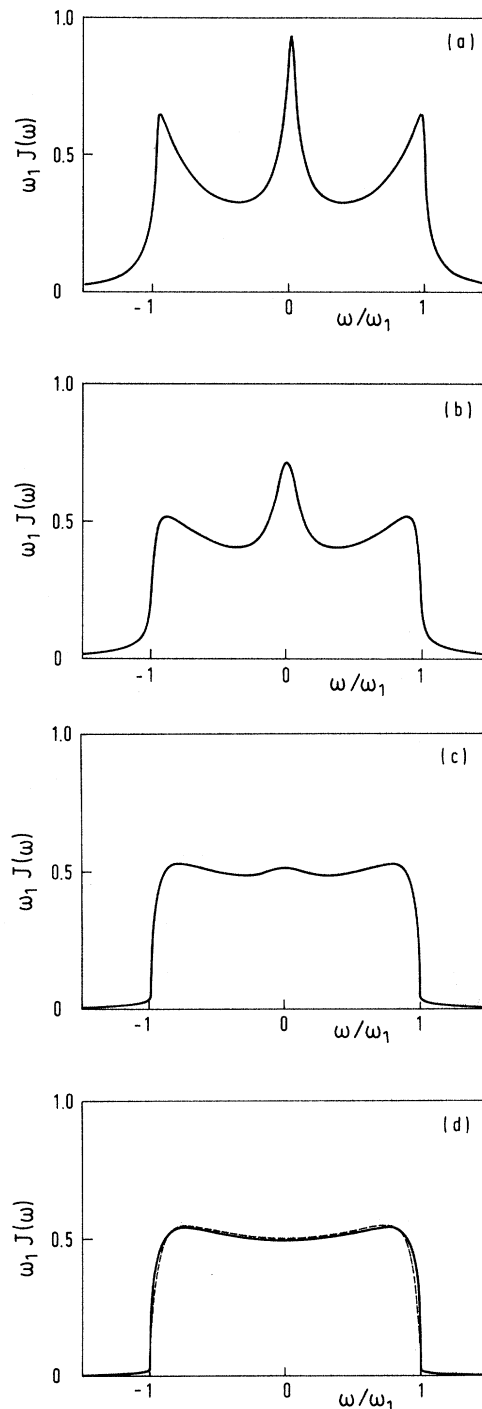


FIG. 3. Same as Fig. 1, but for fixed $X = 10^2$, $T/T_0 = 1.0$, $\tilde{\Delta} = 0.35$, $\tilde{\Omega} = 0.25$, and four different relaxation rates: $\gamma = 2$ (a), 5 (b), 20 (c), and 50 (d). In the limit $\gamma \rightarrow \infty$ the line shape reduces to the static distribution $W(\omega/\omega_1)$, which is given by the Eq. (5.5), and is represented by the dashed line in Fig. 3d.

of magnetic resonance line shapes in proton glasses, which allows us to incorporate the quantum effects of coherent tunneling using the Clauser-Blume model. Here a part of the system is treated quantum mechanically, while the surrounding heat bath is characterized by stochastic forces which cause transitions between quantum states. The static properties of proton glasses, assumed to be given on the level of mean-field theory within the Clauser-Blume model, are described as the static limit of the thermofield-dynamic approach with an instantaneous approximation for the dynamic self-interaction, as in our previous works.^{11,13} An analytic expression for the line shape has been obtained, which is illustrated in Fig. 2 for different values of the tunneling frequency Ω . In the limit of small tunneling ($2\Omega/J \rightarrow 0$) the line shape reduces to the one obtained previously by Pirc *et al.*¹² At low temperatures it consists of a double-peaked distribution, which corresponds to the resonance frequencies of the proton in the left or right equilibrium site, respectively. When the tunneling frequency is different from zero, a third peak at $\omega = 0$ appears. In the limit of large tunneling the intensity of the central peak at $\omega = 0$ increases and the intensity of the two side peaks decreases. The dependence of the line shape on the relaxational frequency λ/ω_1 —measuring the strength of the coupling to the surrounding heat bath—is shown in Fig. 3, whereas the effect of the temperature T/T_0 is illustrated in Fig. 4. An increase of the temperature T/T_0 generally changes the three-peak structure into a single-peaked one. For a very large relaxation rate $\lambda/\omega_1 \rightarrow \infty$, representing the fast motion regime, we find that the line shape is given by the static local-polarization distribution¹³ with p replaced by ω/ω_1 . The effect of the parameter $X = J/2\omega_1$ on the line shape is illustrated in Fig. 5. For small values of X the central line is smeared out, whereas for large values of X a pronounced central peak appears. A typical value of the parameter J in proton glasses is $J/4k_B \approx 60$ K, and $\omega_1 \approx 10^5$ Hz (Ref. 32) for the ^{87}Rb NMR line in D-RADP and 10^8 Hz for the EPR spectrum of Tl^{2+} in RADP.³³

The above results show that a measurement of NMR,

NQR, or EPR line shapes in proton glasses may offer a possibility of discriminating between coherent tunneling processes and incoherent thermally activated jumping of the proton or deuteron across the potential barrier. The

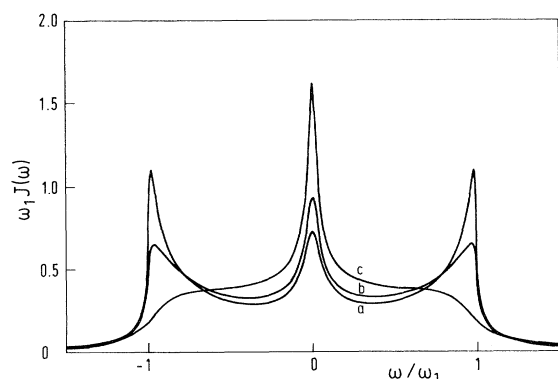


FIG. 4. Same as in Figs. 2 and 3, but for variable temperature $T/T_0 = 0.85$ (a), 1.0 (b), and 1.5 (c), and for fixed $X = 10^2$, $\tilde{\Delta} = 0.35$, $\tilde{\Omega} = 0.25$, and $\gamma = 2.0$.

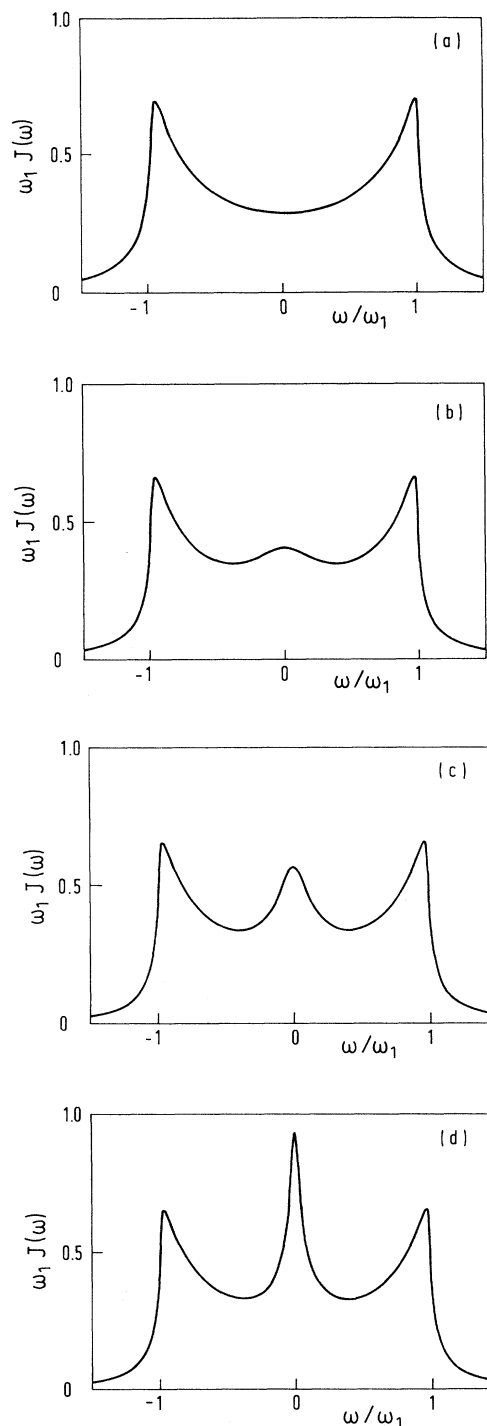


FIG. 5. Same as Figs. 2, 3, and 4, but for fixed $T/T_0 = 1.0$, $\tilde{\Delta} = 0.35$, $\gamma = 2.0$, $\tilde{\Omega} = 0.25$, and various values of the parameter X : 1 (a), 10 (b), 20 (c), and 10^2 (d).

relative strengths of the peak at $\omega = 0$ and the two side peaks permit a quantitative determination of the tunneling frequency.

A few comments are now in order regarding the feasibility of detailed comparison between the theory presented here and resonance experiments of different sorts. It is clear that as the tunneling particle, i.e., the proton or the deuteron, moves from one site to another in an O—H \cdots O bond, it must make a discernible change in the environment for the effect to be detected. How this change is reflected in the corresponding change in the resonance frequency deserves separate remarks for NMR, NQR, and EPR measurements.

Unlike the deuteron the proton has no quadrupole moment and hence, a direct way of tagging the proton spin and performing a proton resonance experiment would be to employ the fact that the chemical shift tensors are different for the two states. However, this effect is expected to be masked by a very broad homogeneous linewidth due to interproton magnetic dipole-dipole coupling which is not significantly altered by the proton transfer. (This is so the interproton distances are much larger than the separation between the two sites in an O—H \cdots O bond.) Therefore, in order to observe fluctuating chemical shift tensors concomitant with the “jump” of the proton, the dipolar interactions must be eliminated by a line narrowing technique, as one does in high-resolution solid-state NMR.³⁴

Still another—though more indirect—way would be to observe the ^{17}O quadrupole resonance line shape. The electric field gradient (EFG) tensor at the ^{17}O in an ^{17}O —H \cdots O hydrogen bond has one value³⁵ when the

proton is “close” to the ^{17}O site and another value²¹ when the proton is in a “far” position. Thus the ^{17}O nuclear quadrupole resonance (NQR) or ^{17}O nuclear quadrupole double resonance³⁵ line shapes reflect the effects of the proton motion and the theory presented in this paper can be directly applied. One advantage of the ^{17}O experiment is that $\Delta\omega = \omega_R - \omega_L$ is expected to be of the order of 10^5 – 10^6 Hz, whereas it is of the order 1–10 Hz for the proton chemical shift experiment in high-resolution NMR in solids.

The above theory can be also applied to electron paramagnetic resonance (EPR) spectra of, e.g., an AsO_4^{4-} center³⁶ where the magnitude of the hyperfine coupling tensor between the electron and proton spins is different if the proton in the O—H \cdots O hydrogen bond is in a close or far position with respect to the unpaired electron, i.e., the AsO_4^{4-} group. The problem with such an experiment is the fact that the unpaired electron in the AsO_4^{4-} group “feels” not only the motion of one proton but the motion of all four protons surrounding a given AsO_4^{4-} group. Still another problem is that the presence of the unpaired electron changes the potential of the O—H \cdots O, so that the obtained results do not reflect the situation in the unperturbed system.

Taking all the above factors into account, high-resolution proton NMR, ^{17}O NQR or double resonance ^{17}O NQR offers the best possibility of testing the present theory and looking for coherent tunneling effects in proton glasses. In spite of the fact that many resonance experiments have been performed for proton and deuteron glasses,³² the relevant experiments to check the above theory have not yet been done, but are highly desirable.

¹E. Courtens, Phys. Rev. Lett. **52**, 69 (1984).

²R. Blinc, D.C. Ailion, B. Günther, and S. Žumer, Phys. Rev. Lett. **57**, 2826 (1986).

³R.A. Cowley, T.W. Ryan, and E. Courtens, Z. Phys. B **65**, 181, (1986).

⁴R. Kind, O. Liechti, and M. Mohr, Ferroelectrics **78**, 87 (1988).

⁵R. Pirc, B. Tadić, and R. Blinc, Z. Phys. B **61**, 69 (1985).

⁶R. Pirc, B. Tadić, and R. Blinc, Phys. Rev. B **36**, 8607 (1987).

⁷T. Yamamoto and H. Ishii, J. Phys. C **20**, 6053 (1987).

⁸B. Tadić, R. Pirc, and R. Blinc, Phys. Rev. B **37**, 679 (1988).

⁹T.K. Kopeć, J. Phys. C **21**, 297 (1988); **21**, 6053 (1988).

¹⁰T.K. Kopeć, K.D. Usadel, and G. Büttner, Phys. Rev. B **39**, 12418 (1989).

¹¹T.K. Kopeć, B. Tadić, R. Pirc, and R. Blinc, Z. Phys. B **78**, 493 (1990).

¹²R. Pirc, B. Tadić, R. Blinc, and R. Kind, Phys. Rev. B **43**, 2501 (1991).

¹³B. Tadić, R. Pirc, and R. Blinc, Physica B **168**, 85 (1991).

¹⁴For an introduction to spin glasses, see, for instance, *Heidelberg Colloquium on Spin Glasses*, edited by J. L. van Hemmen and I. Morgenstern (Springer-Verlag, Berlin, 1983), and D. Chowdhury, *Spin Glasses and Other Frustrated Systems* (World Scientific, Singapore, 1987).

¹⁵An idea of how rich the field is can be obtained from *Ill-*

Condensed Matter, edited by R. Balian, R. Maynard, and G. Toulouse (North-Holland, Amsterdam, 1979).

¹⁶P.G. de Gennes, Solid State Commun. **1**, 132 (1963).

¹⁷R. Blinc and B. Žekš, *Soft Modes in Ferroelectrics and Antiferroelectrics* (North-Holland, Amsterdam, 1974).

¹⁸For the MFT of spin glasses, we refer the reader to K. Binder and A.P. Young, Rev. Mod. Phys. **58**, 801 (1986).

¹⁹A. Abragam, *The Theory of Nuclear Magnetism* (Oxford University Press, London, 1961).

²⁰R. Kubo, J. Phys. Soc. Jpn. **9**, 935 (1954).

²¹P.W. Anderson, J. Phys. Soc. Jpn. **9**, 316 (1954).

²²S. Dattagupta, *Relaxation Phenomena in Condensed Matter Physics* (Academic, Orlando, 1987).

²³M. Blume, Phys. Rev. **174**, 351 (1968).

²⁴M.J. Clouser and M. Blume, Phys. Rev. B **3**, 583 (1971).

²⁵S. Dattagupta, Phys. Rev. B **16**, 158 (1977).

²⁶For very general conditions under which a double well can be mapped onto a TLS, see, for instance, A.J. Leggett, S. Chakravarty, M.P.A. Fisher, A.T. Dorsey, A. Garg, and W. Zwerger, Rev. Mod. Phys. **59**, 1 (1987).

²⁷We should emphasize that I^z has nothing to do with the actual spin of the nucleus being probed in NMR and NQR experiments, which usually has a value greater than $\frac{1}{2}$. In that sense, I^z is another pseudospin, introduced here as a mathematical construct, in order to account for resonance transitions.

²⁸R.J. Glauber, J. Math. Phys. **4**, 294 (1963).

- ²⁹H.J. Sommers, Phys. Rev. Lett. **58**, 1268 (1987).
- ³⁰See, for instance, A. Messiah, *Quantum Mechanics* (North-Holland, Amsterdam, 1965), Vol. II, Chap. XIII.
- ³¹H. Umezawa, H. Matsumoto, and M. Tachiki, *Thermofield Dynamics and Condensed States* (North-Holland, Amsterdam, 1982).
- ³²R. Blinc, J. Dolinšek, R. Pirc, B. Tadić, B. Zalar, R. Kind, and O. Liechti, Phys. Rev. Lett. **63**, 2248 (1989).
- ³³R. Kind, R. Blinc, J. Dolinšek, N. Korner, B. Zalar, P. Cevc, N.S. Dalal, and J. DeLooze, Phys. Rev. B **43**, 2511 (1991).
- ³⁴See, for instance, M. Mehring, *High Resolution NMR Spectroscopy in Solids*, 2nd ed. (Springer, Berlin, 1983).
- ³⁵R. Blinc, Z. Naturforsch. **41a**, 249 (1986).
- ³⁶R. Blinc, P. Cevc, and M. Schara, Phys. Rev. **159**, 411 (1967).